Evaluation of Coatings for Mg Alloys for Biomedical Applications**

By *Nor Ishida Zainal Abidin, Anna Da Forno, Massimiliano Bestetti, Darren Martin, Aiden Beer* and *Andrej Atrens**

Received: November 6, 2013
Final Version: March 20, 2014
Published online: April 25, 2014

1. Introduction

Biodegradable medical implant applications is a relatively new area where there is significant interest in Mg alloys[1–13] because Mg alloys would corrode away, completely obviating the necessity for a second surgery to remove the implant after it had completed its function. Mg alloys are attractive because of their good mechanical properties. They have adequate strength and ductility, and have stiffness close to that of human bone. Their corrosion properties are an advantage, whereas corrosion typically limits applications in aggressive chloride containing solutions.[1,2,14–19] The study of Mg corrosion is made complicated by the fact that Tafel extrapolation of polarization curves often does not work for Mg alloys[1,14,20] despite the fact that this is a standard electrochemical technique.

Mg alloys corrode relatively quickly in chloride containing solutions[1,2,14–26] because (i) the surface corrosion films provide little inhibition to the large driving force for corrosion because of the active nature of Mg, and (ii) second phases in Mg alloys accelerate corrosion by micro-galvanic coupling to the Mg matrix. In technically relevant testing solution like 3.5% NaCl, all Mg alloys corrode faster than high-purity (HP) Mg. Low-purity (LP) Mg with an Fe impurity content above 180 ppm typically corrodes orders of magnitude faster than HP Mg.

The corrosion rates of existing Mg alloys are somewhat higher than would be liked for biodegradable medical applications. The only effective alloying strategy is to identify an alloying element that would produce a more protective surface film, such as Cr in stainless steels, nickel, and cobalt base alloys, where Cr alloying produces low corrosion

[*] *A. Atrens, N. I. Zainal Abidin*
Division of Materials, The University of Queensland, St Lucia, Qld 4072, Australia
E-mail: andrejs.atrens@uq.edu.au
N. I. Zainal Abidin
Faculty of Engineering, Department of Mechanical Engineering, University of Malaya, Kuala Lumpur 50603, Malaysia
A. Da Forno, M. Bestetti
Politecnico di Milano, Dipartimento di Chimica, Materiali e Ingegneria Chimica, Via Mancinelli, 7, 20131 Milano, Italy
D. Martin
Australian Institute for Bioengineering and Nanotechnology, The University of Queensland, Brisbane, Qld 4072, Australia
A. Beer
Institute for Frontier Materials, Deakin University, Wuarn Ponds, Vic 3216, Australia

[**] *CAST CRC supported this project. CAST CRC was established under, and was supported in part by, the Australian Government's Cooperative Research Centres scheme.*

rates[27–35] above a critical Cr concentration by means of a more stable passive film. This strategy so far is not successful for Mg alloys.

The other feasible possibility to decrease the effective corrosion rate is to use a surface coating. As a consequence, coatings on Mg alloys have received considerable attention.[36–62] To our knowledge, no composites anodic oxide + silane coating have been evaluated for biodegradable applications. For that purpose, a number of coatings were developed for this work based on the prior promising results[63]: (i) anodization, (ii) silanes, and (iii) anodization + silane.

The research aims were as follows.

To compare the corrosion rates of uncoated HP Mg and ME10, and coated HP Mg and ME10 in Nor's solution, and to use the new fishing-line specimens[17] to understand the corrosion behavior of coated HP Mg and ME10 to be used in medical applications.

2. Experimental Methods

2.1. Materials

This research used as-cast HP Mg and extruded ME10. HP Mg has lowest corrosion rate for any Mg alloy. ME10 may have a corrosion rate lower than other Mg alloys, and still have improved strength and ductility, better than that of HP Mg. HP Mg was as used in our prior research;[2,7,13,17–19] it had a low concentration of impurities below their tolerance limit.[25] ME10, a dilute, rare-earth containing Mg alloy (with a nominal composition of 1 wt% Mn and 0.2 wt% La) was developed for good mechanical properties with enhanced extrudability, significantly better than and that of common wrought magnesium alloys with comparable mechanical properties.[64] The blanks for the coated specimens were machined into the shape and dimensions as shown in Figure 1: $a = 3$ mm, $b = 3$ mm, $c = 10$, and 1.5 mm hole diameter. The uncoated specimens were machine cut into the same shape and dimensions without the hole. The specimens were washed in stirred chromic acid solution made with 200 g L^{-1} CrO_3 + 10 g L^{-1} $AgNO_3$ to remove surface oxides and machining residues. This cleaning solution has been shown to remove no metallic Mg as it removes the corrosion products[65–67] The specimens were then washed with distilled water, dried, and kept in the desiccator until needed for immersion testing or the coating was applied.

2.2. Coatings

For the production of anodized coatings, the specimens were anodized at 130 V at room temperature in alkaline electrolyte consisting of 100 g L^{-1} sodium phosphate, 25 g L^{-1} sodium borate, and 20 g L^{-1} sodium metasilicate. Two AISI 316 stainless steel panels were the cathodes. During anodizing, the cell voltage was increased linearly to the maintenance voltage in a fixed time ramp of 120 s, and then the cell voltage was maintained constant. The total anodizing time was 5 min.

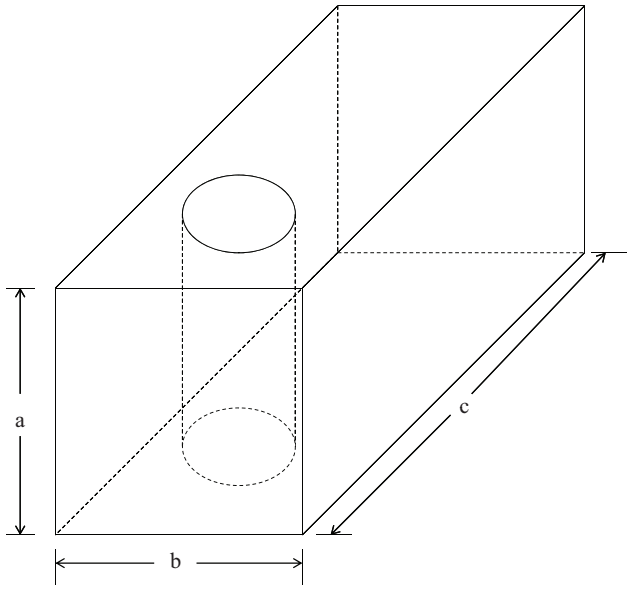

Fig. 1. Specimen shape and dimensions.

Anodizing can be useful to modulate the corrosion rate. As these anodized coatings are porous and cracked a sealing treatment is required.

Two silanes were used. Octyltrimethoxysilane, designated as OSi, has the following chemical formula $CH_3(CH_2)$ $6CH_2$–Si–$(OCH_3)_3$. BTSE is the designation for 1,2-bis[triethoxysilyl] ethane (BTSE), a commercial product, which has the chemical formula $(H_5C_2O)_3Si(CH_2)_2Si(OC_2H_5)_3$. Each silane was used as a 4% silane solution in 95:5 methanol:water, with the pH adjusted to 4.3 by the addition of 10 vol% acetic acid. Silane coatings were produced by dipping a specimen for 30 s in the silane solution, drying in a hot-air stream, and curing in an open-to-air sand oven for 30 min at 110 °C. The OSi silane treatment was applied on HP Mg and ME10. Both OSi and BTSE silane treatments were applied to anodized HP Mg and ME10.

2.3. Specimen Characterization

Surface morphology of specimens anodized, anodized and silane coated, and coated only with silane were observed by scanning electron microscopy (SEM Zeiss EVO 50EP microscope at a chamber pressure of 50 Pa and 20 kV accelerating voltage) coupled with energy dispersive X-rays spectroscopy (EDS).

2.4. Immersion Test

The immersion test arrangement is illustrated in Figure 2 as per our prior research.[2] Each specimen was weighed, to give the specimen weight before immersion, W_b (mg). The specimen was hung with fishing line for 7–14 days in a beaker at 37 ± 2 °C in 0.7 L Nor's solution, which is the designation given to CO_2-bicarbonate buffered Hank's solution. The Hank's solution was made using Hank's balanced salt (without sodium bicarbonate and phenol red, Sigma–Aldrich), sodium bicarbonate (reagent grade), and

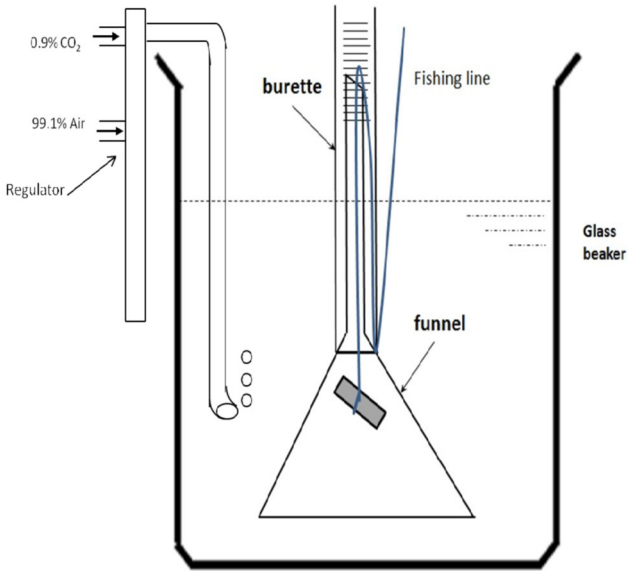

Fig. 2. Experimental arrangement for corrosion measurement during an immersion test with a fishing line specimen. Carbon dioxide (CO_2) at 0.009 atm partial pressure was bubbled through the solution throughout the immersion test.

distilled water. The chemical composition of Hank's solution is shown in Table 1.[68] CO_2 (supplied by Coregas Pty Ltd.) at partial pressure of 0.009 atm was bubbled through the solution throughout the immersion test to maintain constant the solution pH. The fishing line specimen was used to evaluate the corrosion rate by (i) hydrogen evolution and (ii) weight loss over the whole duration of immersion. During immersion, each atom of corroded Mg evolves one molecule of hydrogen according to:[1,14,15]

$$Mg + 2H_2O \rightarrow 2OH^- + H_2 \quad (1)$$

The evolved hydrogen was collected into the burette above the corroding Mg specimen.

2.5. Corrosion Evaluation

The corrosion rate, P_H (mm year^{-1}) of each specimen was evaluated from the evolved hydrogen volume collected from the corroding Mg specimen, which was converted to the standard temperature (0 °C) and pressure (1 atm) using the ideal gas law. The hydrogen evolution rate, V_H (mL cm^{-2} d^{-1}), was obtained from the evolved hydrogen volume by dividing by the immersion time. The corrosion rate averaged over the immersion time, P_H (mm year^{-1}), was evaluated from refs.:[1,2,17]

$$P_H = 2.279 V_H \quad (2)$$

After the immersion test, each specimen was cleaned in the chromic acid solution made from 200 g L^{-1} CrO_3 + 10 g L^{-1} $AgNO_3$ for 40 min in an ultrasonic bath to remove the corrosion products and coating residues after the immersion test. This cleaning solution removes surface oxide without removing the any amount of metallic Mg.[1,2,17] The specimen was washed with distilled water, dried in the desiccator for 1–2 days and weighed, to give the specimen weight after the immersion test and after removal of corrosion products, W_a (mg).

For uncoated specimens, the weight loss rate, W_L was obtained using:[1,2,17]

$$W_L = \frac{W_b - W_a}{A t_L} \quad (3)$$

where A was the specimen surface area (cm^2) and t_L was the total immersion time (d).

This quantity was also evaluated for the coated specimens. However, for the coated specimens, the weight before the immersion tests was equal to the weight of the Mg specimen, $W_{b,s}$, plus weight of the coating, $W_{b,c}$, so that:

$$W_b = W_{b,s} + W_{b,c} \quad (4)$$

whereas the weight of the specimen after the immersion tests and after removal of the corrosion products was purely the weight of the specimen, because the coating had been removed. Thus, the weight loss rate, W_L, as evaluated by Equation (3) includes the decrease in the weight of Mg lost as well as the weight of the coating. The data could not be deconvoluted to separate the results of weight loss and the weight of the coating. Thus, this data is not reported.

For the uncoated samples, the average corrosion rate P_W (mm year^{-1}) was obtained from:[1,2,17]

$$P_W = 2.1 W_L \quad (5)$$

Each specimen surface appearance after the immersion and after acid cleaning was documented with a digital camera.

3. Results

3.1. Coating Characterization

The anodic oxides grown in the micro-arc regime are porous regardless of the solution composition, however, SEM

Table 1. Chemical composition in terms of ions of Hank's solution compared with the inorganic part of human blood plasma.

	Composition in terms of ions [mmol L^{-1}]									
Solution	Na^+	K^+	Mg^{2+}	Ca^{2+}	Cl^-	HCO_3^-	$H_2PO_4^-$	HPO_4^{2-}	SO_4^{2-}	Refs.
Hank's	142	5.8	0.8	2.5	145	4.2	0.4	0.3	0.8	This work
Blood plasma	142	3.6–5.5	1.0	2.1–2.6	95--107	27	–	0.7–1.5	1.0	65

images (Figure 3) and EDS spectra of anodized HP Mg (left) and ME10 alloy (right) show a quite different morphology depending on the substrate. As evident in these images, onto HP Mg substrate some uncoated areas were present whereas the coating onto ME10 alloy showed the typical morphology of oxides grown in micro-arc anodic oxidation. Moreover, only the oxide grown onto ME10 presented the fused aspect due to the high temperatures reached within the plasma.[69] Verdier *et al*.[69] suggested that the pores are likely the traces of the sparks, and the round shape structures are the result of bubbles expelled from the oxide during fusion, solidified after cooling. In contrast, on HP Mg the oxide was porous, but round shape structures were less evident. Figure 3 shows the EDS spectra of HP Mg oxide (left) and ME10 oxide (right). These spectra show that (i) the signals of silicon and phosphorus were similar for both the oxides, (ii) signals of oxygen and magnesium were roughly equivalent for the oxide grown onto HP Mg, and (iii) the signal of oxygen was almost twice than that of magnesium. The higher O/Mg ratio in the case of ME10 indicated that the oxide grown on ME10 was thicker than that onto HP Mg, in agreement with the SEM observations.

Figure 4 shows the surface morphologies and EDS spectra of HP Mg anodized and silane coated with OSi (left) and BTSE (right). As shown in Figure 4 (left), the uncoated areas were more numerous compared to those of the anodized specimen (Figure 3, left). The reason was attributed to the pH 4.3 of the solution used for silane deposition and a higher aggressiveness of OSi in comparison with BTSE solution. EDS spectra show in both cases quite similar values of peak intensities.

Figure 5 shows the surface morphologies and EDS spectra of ME10 anodized and silane coated with OSi (left) and BTSE (right). As shown in this figure, the surface morphologies of the two different silane-based coatings onto anodized ME10 were similar and had similar ratios O/Mg.

Figure 6 shows the surface morphologies and EDS spectra of HP Mg coated with OSi (left) and BTSE (right) without any oxidation pretreatment. As the silane deposition produced a nanosized layer, the polishing lines were evident. The EDS spectra show the presence of silicon, not detected on the bare substrate.

Figure 7 shows the surface morphologies and EDS spectra of ME10 coated with OSi (left) and BTSE (right) without any oxidation pretreatment. The same comments as for HP Mg were also reasonable for ME10.

3.2. Corrosion Evaluation

The corrosion behavior of specimens immersed in Nor's solution at 37 °C for 7–14 days was characterized by the

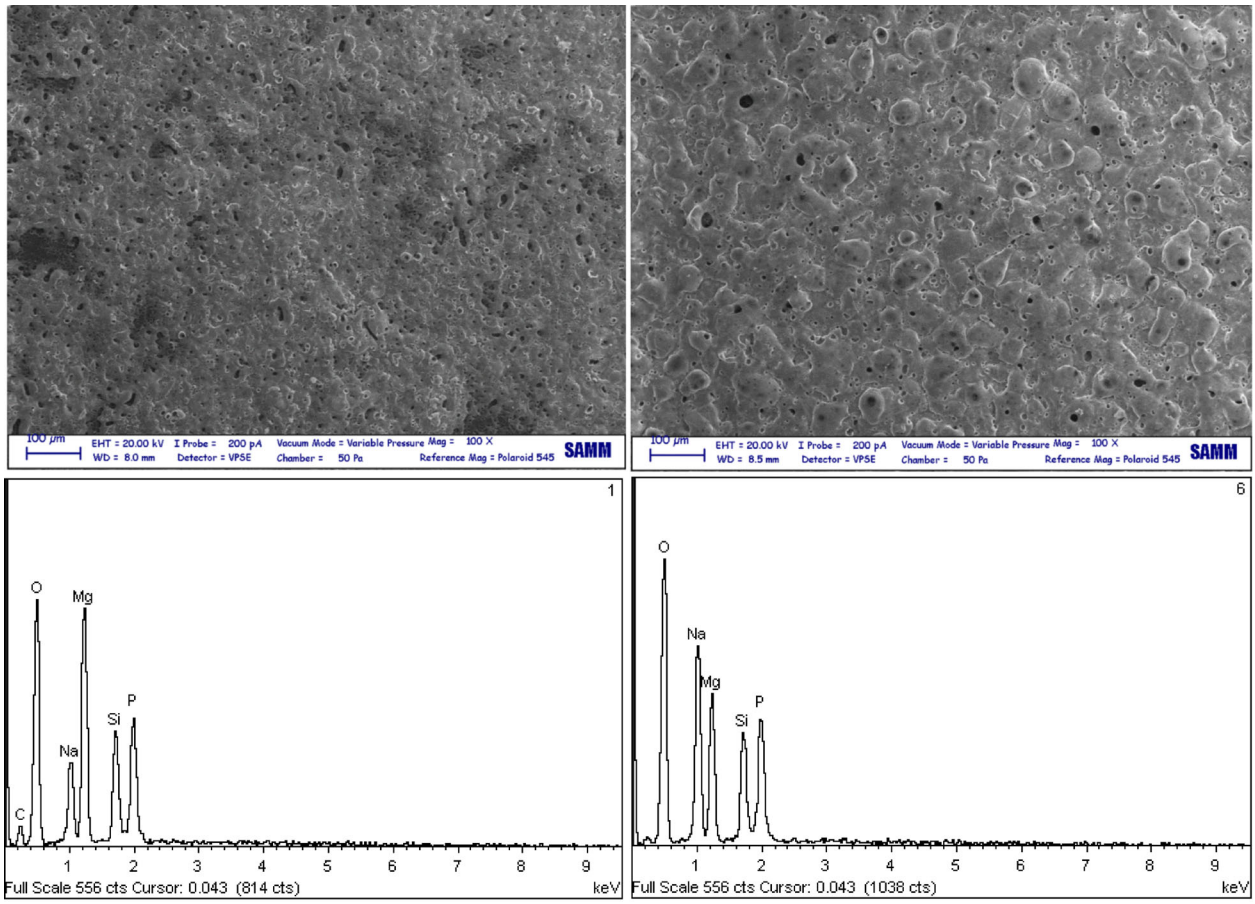

Fig. 3. SEM surface morphologies and EDS spectra of anodized HP Mg (left) and ME10 (right).

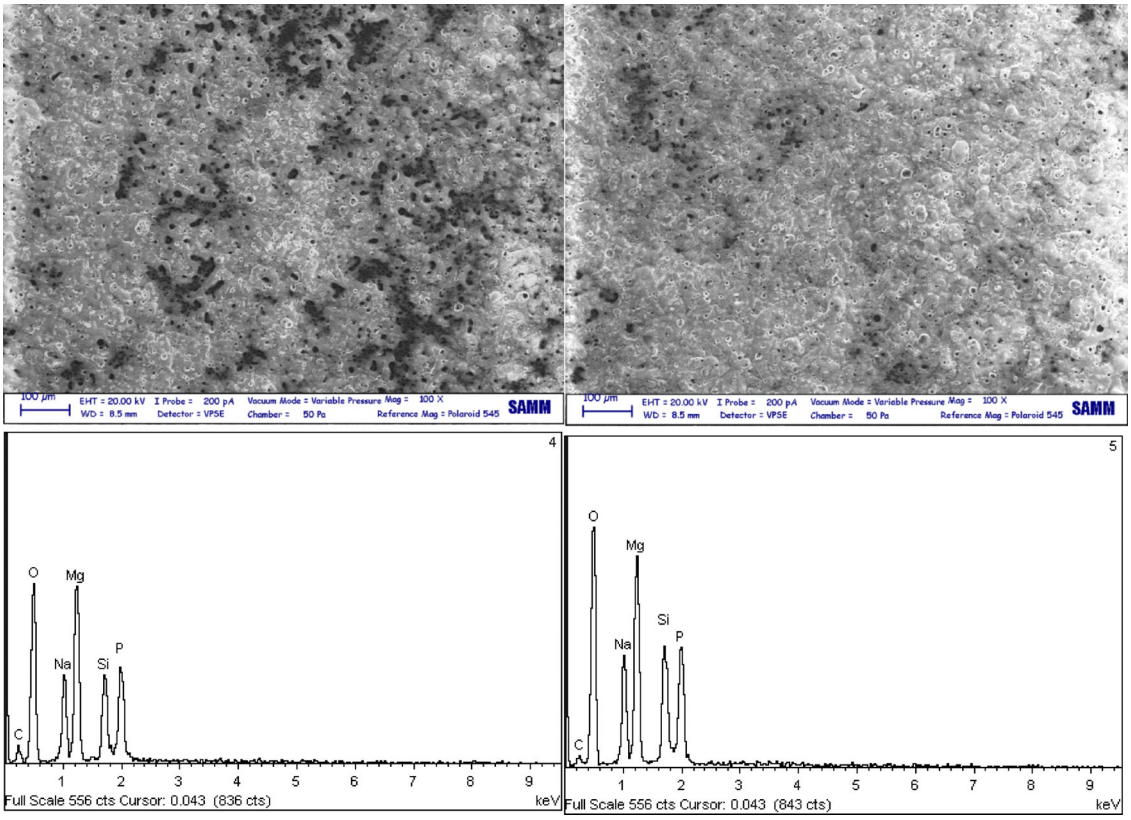

Fig. 4. Surface morphologies and EDS spectra of HP Mg anodized and coated with OSi (left) and BTSE (right).

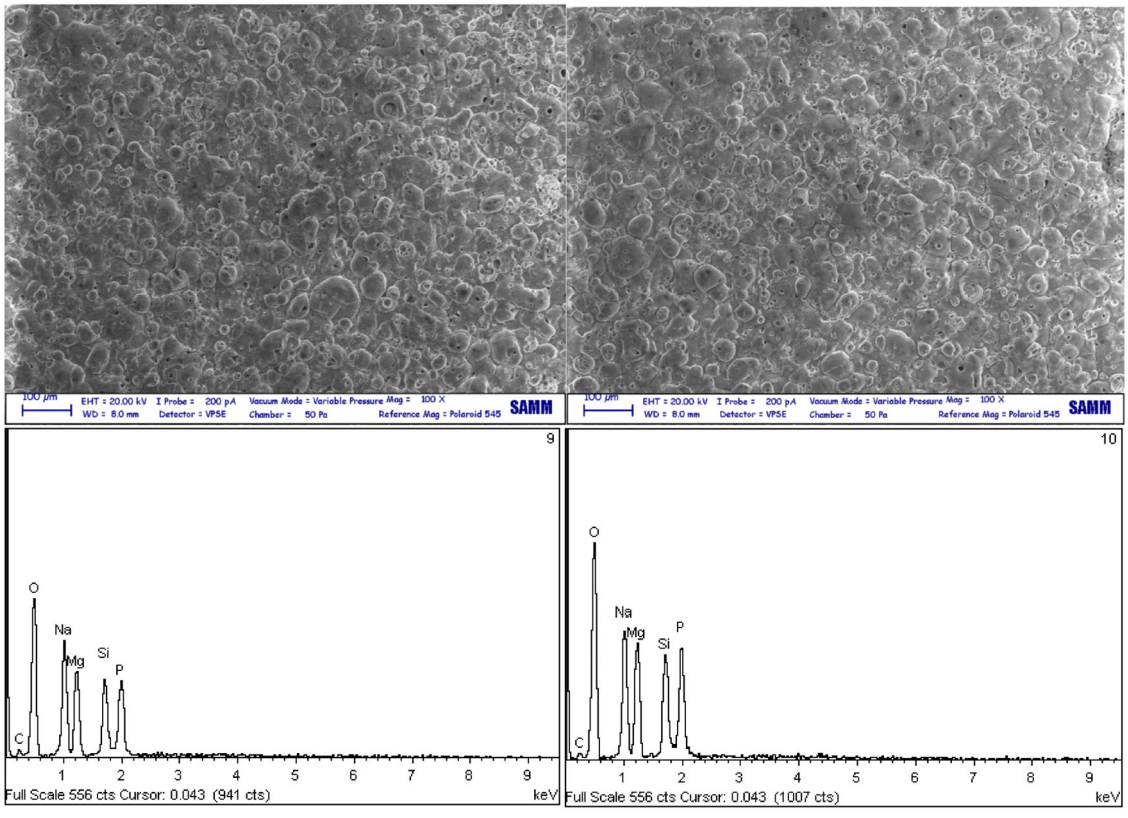

Fig. 5. Surface morphologies and EDS spectra of ME10 anodized and coated with OSi (left) and BTSE (right).

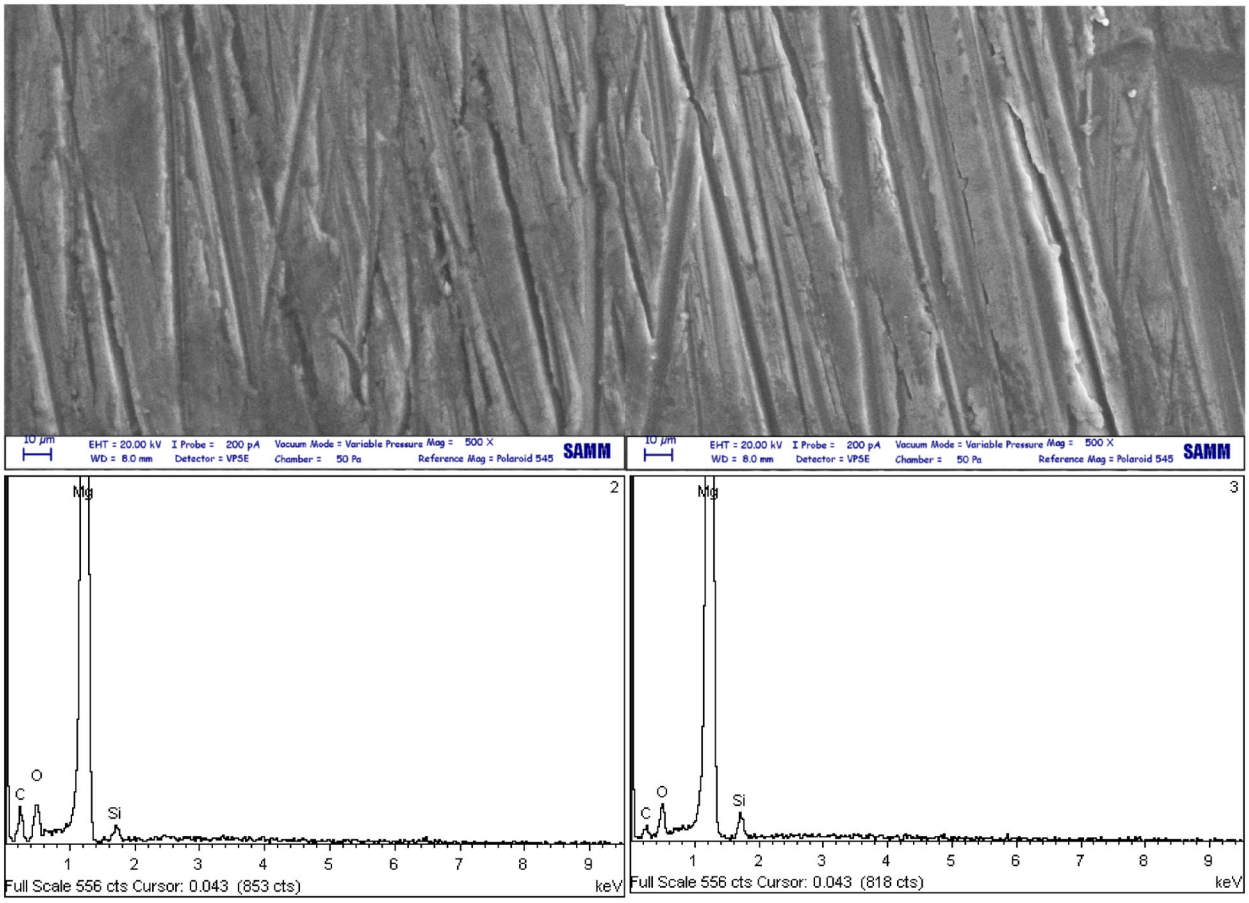

Fig. 6. Surface morphologies and EDS spectra of HP Mg coated with OSi (left) and BTSE (right).

evolved hydrogen for all specimens, and weight loss rate for the uncoated specimens.

Figure 8 presents the hydrogen evolution volume as open symbol, and the corresponding pH of the solution is given by the corresponding full symbols. Duplicate specimens were used for each material; these were designated as 1 and 2. The hydrogen evolution data for HP Mg anodized 2, HP Mg OSi 2, ME10 OSi 2, and HP Mg anodized + BTSE 2 specimens could not be reported because some CO_2 bubbles entered into the funnel and were collected by the burette. The measurements errors were smaller than the size of the symbols. Thus, the variation shown is due to variations in corrosion performance of the Mg specimens.

Figure 8 shows that the hydrogen evolution volume increased with the immersion time.

Table 2 presents the corrosion rates evaluated from the weight loss rate for the uncoated specimens. Also included in Table 2 are the corrosion rates evaluated from the hydrogen evolution data of Figure 8 for each specimen (i) averaged over 120 h, $P_{120\,h,\,H}$, and (ii) the average corrosion rate over the total of immersion time, P_{AH}. The average corrosion rates obtained from the hydrogen evolution volume, P_{AH}, were smaller than the corrosion rates obtained from the weight loss, P_W for all the specimens. This is consistent with a significant amount of hydrogen dissolving in the Mg specimen as in our prior research.[2,18] It means that the corrosion rates as evaluated by hydrogen evolution must be considered as indicative only, and can only be used to compare the behavior of the coated specimens to their uncoated counterparts. There was good consistency and repeatability between the duplicate specimens.

Figure 8a indicates that the hydrogen evolution volume increased steadily with immersion time for uncoated HP Mg and uncoated ME10 with no incubation period for all uncoated HP Mg and uncoated ME10 specimens. The hydrogen evolution rate was similar for HP Mg and ME10.

Figure 8b shows that the hydrogen evolution for the anodized specimens was similar to that for the uncoated specimens, although the hydrogen evolution rate for specimen ME10 anodized 2 was slower than for uncoated ME10.

Figure 8c shows that the hydrogen evolution rates for HP Mg OSi 1 and ME10 OSi 1 were slower than for uncoated HP Mg and uncoated ME10.

Figure 8d presents the hydrogen evolution volume for specimens that had been anodized and coated with OSi. There was an incubation period for all specimens. The incubation period was longer for ME10 anodized + OSi. Moreover, the hydrogen evolution rate for ME10 anodized + OSi was slower than for uncoated ME10. In contrast, the hydrogen evolution rate for HP Mg anodized + OSi was comparable to that for uncoated HP Mg.

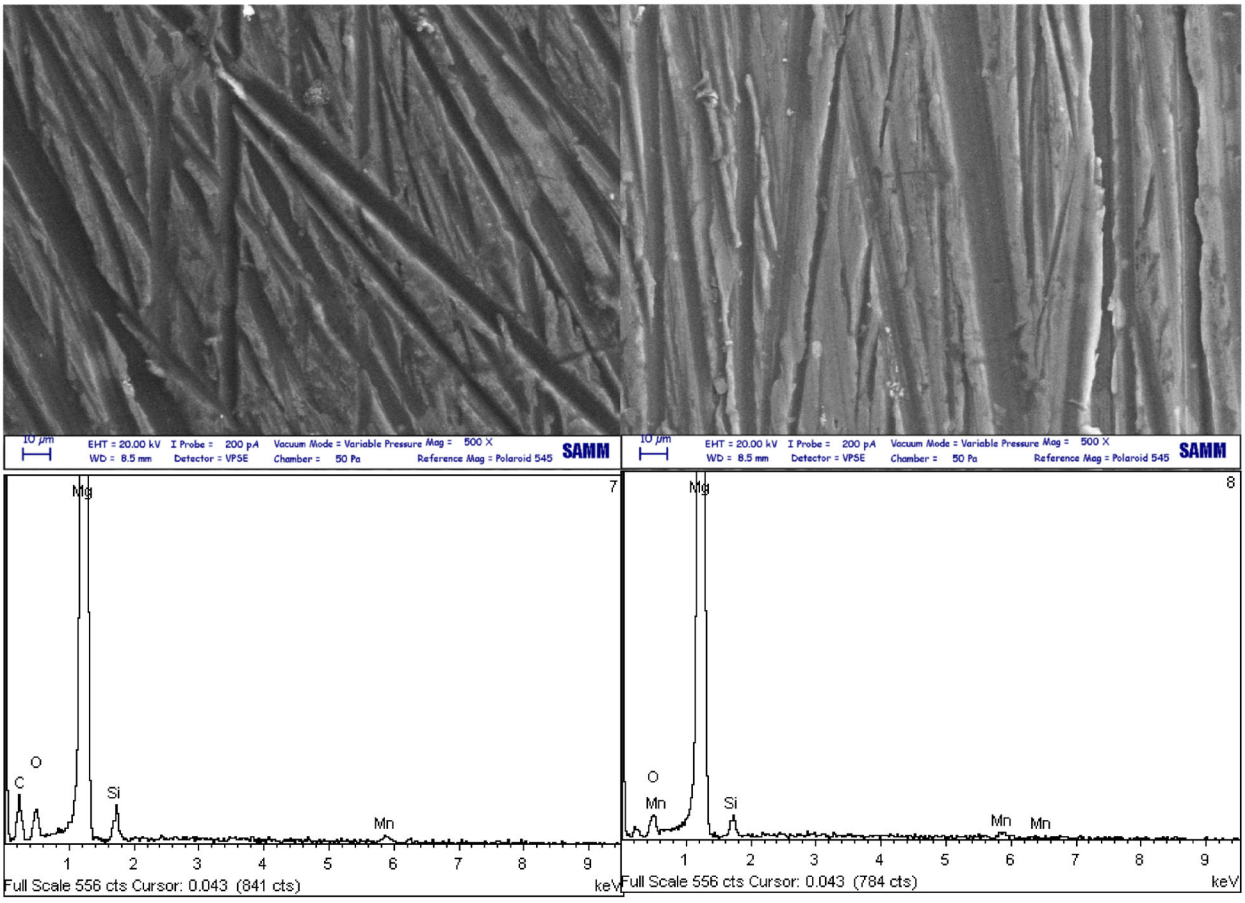

Fig. 7. Surface morphologies and EDS spectra of ME10 alloy coated with OSi (left) and BTSE (right).

Figure 8e presents the hydrogen evolution data for specimens that had been anodized and coated with BTSE. The hydrogen evolution rates for HP Mg anodized + BTSE 1 and ME10 anodized + BTSE 2 were smaller than for uncoated HP Mg and ME10, whereas the hydrogen evolution rate for ME10 anodized + BTSE 2 was comparable to that for uncoated ME10.

3.3. Solution pH

The pH value of each of the Nor's solution during each immersion experiment was recorded throughout the immersion test. The pH value is shown as full symbols in Figure 8. The pH was successfully maintained in the 6.5–7.5 range by bubbling through the Hank's solution CO_2 with a partial pressure of 0.009 atm throughout the experiment.

3.4. Corroded Surface Evaluation

The surface appearance was characterized for each specimen after the immersion test, and also after removal of the corrosion products. The surface appearance of (uncoated) HP Mg 2 (which had a slightly higher corrosion rate than HP Mg 1) was characterized by superficial corrosion with some deeper heterogeneous corrosion in few areas. The surface appearance after corrosion products removal of uncoated ME10 1 indicated superficial heterogeneous corrosion all over the surface. The surface appearance after removal of the corrosion products (and the coatings) for the coated samples was similar to that of the uncoated samples, except that there was some indication of some deeper heterogeneous corrosion in some cases.

4. Discussion

4.1. Corrosion Evaluation

The corrosion behavior of each specimen was evaluated by the weight loss as presented in Table 2 and hydrogen evolution recorded throughout the immersion test as presented in Figure 8 and summarized in Table 2.

The corrosion rates of uncoated HP Mg obtained from weight loss, P_W, were consistent with previous measurements in 3.5% NaCl saturated $Mg(OH)_2$[17–19] and in Nor's solution at 37 °C,[2] giving confidence in the present measurements. The corrosion rate of the uncoated ME10 was similar to that of uncoated HP Mg. This is attributed to the fact that ME10 is a relatively lean alloy, with only a small concentration of alloying additions (and only small precipitates) that did not adversely influence the corrosion behavior.

The average corrosion rates obtained from the hydrogen evolution volume, P_{AH}, were smaller than the corrosion rates obtained from the weight loss, P_W for all the specimens. This

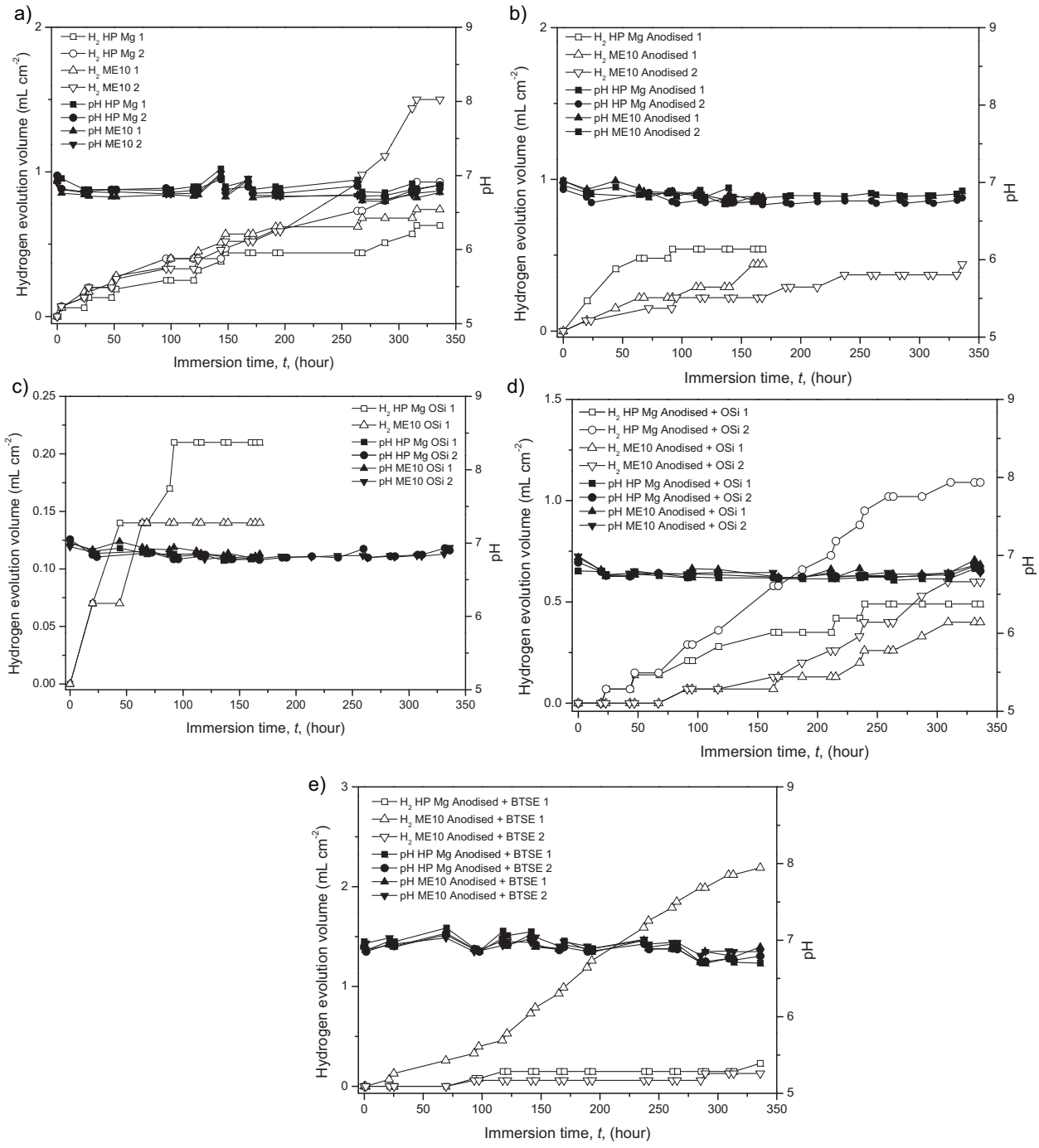

Fig. 8. (a) Solution pH (full symbols) and corrosion behavior as characterized by hydrogen evolution (open symbols) during the immersion tests for HP Mg and ME10. (b) Solution pH (full symbols) and corrosion behavior as characterized by hydrogen evolution (open symbols) during the immersion tests for HP Mg anodized and ME10 anodized. (c) Solution pH (full symbols) and corrosion behavior as characterized by hydrogen evolution (open symbols) during the immersion tests for HP Mg OSi and ME10 OSi. (d) Solution pH (full symbols) and corrosion behavior as characterized by hydrogen evolution (open symbols) during the immersion tests for HP Mg anodized + OSi and ME10 anodized + OSi. (e) Solution pH (full symbols) and corrosion behavior as characterized by hydrogen evolution (open symbols) during the immersion tests for HP Mg anodized + BTSE and ME10 anodized + BTSE.

means that a significant amount of hydrogen dissolved in the Mg specimen as in our prior research.[2,18] If a straight line could be drawn through the data, then the slope of the line is much smaller than in our prior research.[2] This might indicate that hydrogen enters into HP Mg at pH 7 much easier than into the Mg alloys studied previously,[2] and into HP Mg in 3.5% NaCl saturated with $Mg(OH)_2$.

4.2. Performance of Coated Specimens

The data of Figure 8 and Table 2 showed that the corrosion rates of the coated specimens were similar to or lower than that of the uncoated specimens. The corrosion rate was lower for (i) ME10 anodized 2, (ii) HP Mg OSi 1 and ME10 OSi 1, (iii) ME10 anodized + OSi, and (iv) HP Mg anodized + BTSE 1 and ME10 anodized + BTSE 2.

Table 2. Corrosion performance for uncoated and coated HP Mg and ME10.

Specimen	$P_{120\ h,H}$ [mm year^{-1}]	P_{AH} [mm year^{-1}]	P_W [mm year^{-1}]
HP Mg 1	0.10	0.09	0.48
HP Mg 2	0.15	0.13	0.62
ME10 1	0.15	0.11	0.55
ME10 2	0.13	0.22	0.63
HP Mg anodized 1	0.18	0.15	
HP Mg anodized 2			
ME10 anodized 1	0.10	0.13	
ME10 anodized 2	0.08	0.06	
HP Mg OSi 1	0.07	0.06	
HP Mg OSi 2			
ME10 OSi 1	0.04	0.04	
ME10 OSi 2			
HP Mg anodized + OSi 1	0.11	0.07	
HP Mg anodized + OSi 2	0.17	0.16	
ME10 anodized + OSi 1	0.03	0.06	
ME10 anodized + OSi 2	0.04	0.09	
HP Mg anodized + BTSE 1	0.06	0.03	
HP Mg anodized + BTSE 2			
ME10 anodized + BTSE 1	0.20	0.31	
ME10 anodized + BTSE 2	0.03	0.02	

Anodization is known to typically produce a somewhat porous coating, which can nevertheless passivate the Mg surface[39–43]; this can produce specimens with a corrosion rate lower than the uncoated counterpart as, for example, was the case for ME10 anodized 2. Nevertheless, coatings produced by anodization are often sealed or covered with a second coating in order to enhance corrosion resistance. In this research, silanes were used to seal the coatings produced by anodization. After hydrolysis, reaction chemical bonds form between the –OH groups of the silane and $Mg(OH)_2$ by means of a condensation reaction and elimination of water.[63]

As shown in Table 2, corrosion rate of the anodized ME10 specimens was lower than that of anodized HP Mg. These results were consistent with SEM images of Figure 3 and 4 that showed a more homogeneously coated surface and a higher thickness of ME10 oxide in comparison with the HP Mg oxide. Similarly, corrosion rates of HP Mg anodized and coated with OSi and BTSE were in agreement with the surface morphology images of Figure 4. The lower corrosion rate of specimens coated with BTSE were attributed to a better uniformity of the coating as shown in Figure 4 (right).

ME10 samples anodized and coated with OSi have a low corrosion rate while for those coated with BTSE the results were variable.

According to the results of Table 2, also the corrosion rates of HP Mg and ME10 coated with OSi were low, and the anodic oxide as interlayer between the substrate and the silane-based coating was fundamental to improved properties of the system.

The OSi silane coating by itself gave promising results, and together with anodization the corrosion rates for ME10 anodized + OSi specimens were lower than for the uncoated specimens. Particularly promising was the substantial initial period of low corrosion rate as evident from Figure 8d. Similarly, there were promising results for HP Mg anodized + BTSE 1, and ME10 anodized + BTSE 2.

Treatments with hydro-alcoholic solutions of silanes, following the classical steps of immersion and curing, have been used mainly on bare magnesium alloys. In this work, the silane-based treatment has been used to seal the pores typical of the anodic oxides grown in the micro-arc regime. As in our previous research carried out on AM60B magnesium alloy,[63] the silane-based coatings obtained by means of OSi as precursor provided a better barrier action against corrosion in comparison with BTSE. In the previous work, SEM examination of anodized + OSi and anodized + BTSE samples showed that OSi penetrated deeper into the pores and cracks generated during the anodizing process. Due to inhibition of magnesium dissolution, the more hydrophobic OSi provided a better anchorage to the substrate. The results achieved in the present investigation agreed with those achieved in our previous research.[63]

5. Conclusions

1) The CO_2 bubbled at partial pressure of 0.009 atm through the solution successfully maintained the solution pH throughout the experiment.
2) The performance of coated samples was comparable to or better than that of the uncoated samples.
3) ME10 that had been anodized and coated with OSi showed promise for use in medical application as the corrosion rate from the hydrogen evolution were lower than that of uncoated HP Mg.
4) Corrosion performance of HP Mg and ME 10, as measured by means of hydrogen evolutions tests, was in agreement with the morphologies observed at SEM.
5) Some of the evolved hydrogen was dissolved in the Mg metal.

[1] A. Atrens, M. Liu, N. I. Zainal Abidin, *Mater. Sci. Eng. B* **2011**, *176*, 1609.
[2] N. I. Zainal Abidin, A. D. Atrens, D. Martin, A. Atrens, *Corros. Sci.* **2011**, *53*, 3542.
[3] S. Virtanen, *Mater. Sci. Eng. B* **2011**, *176*, 1600.
[4] F. Witte, *Acta Biomater.* **2010**, *6*, 1680.
[5] B. Zberg, P. J. Uggowitzer, J. F. Loeffler, *Nat. Mater.* **2009**, *8*, 887.
[6] S. Remennik, I. Bartsch, E. Willbold, F. Witte, *Mater. Sci. Eng. B* **2011**, *176*, 1653.

[7] N. I. Zainal Abidin, B. Rolfe, H. Owen, J. Malisano, D. Martin, J. Hofstetter, P. J. Uggowitzer, A. Atrens, *Corros. Sci.* **2013**, *75*, 354.

[8] A. C. Hänzi, I. Gerber, M. Schinhammer, J. F. Löffler, P. J. Uggowitzer, *Acta Biomater.* **2010**, *6*, 1824.

[9] H. Kalb, A. Rzany, B. Hensel, *Corros. Sci.* **2012**, *57*, 122.

[10] Y. L. Zhou, D. M. Luo, W. Y. Hu, Y. Li, P. Hodgson, C. Wen, *Adv. Sci. Lett.* **2011**, *4*, 2860.

[11] T. Kraus, S. F. Fischerauer, A. C. Hänzi, P. J. Uggowitzer, J. F. Loffler, *Acta Biomater.* **2012**, *8*, 1230.

[12] M. Carboneras, M. C. Garcia-Alonso, M. L. Escudero, *Corros. Sci.* **2011**, *53*, 1433.

[13] C. Taltavull, Z. Shi, B. Torres, J. Rams, A. Atrens, *J. Mater. Sci. : Mater. Med.* **2014**, *25*, 329.

[14] G. L. Song, A. Atrens, *Adv. Eng. Mater.* **2003**, *5*, 837.

[15] G. L. Song, A. Atrens, *Adv. Eng. Mater.* **1999**, *1*, 11.

[16] A. Atrens, M. Liu, N. I. Zainal Abidin, G. Song, in *Corrosion of Magnesium Alloys* (Ed: G. L. Song), Woodhead, Cambridge, **2011**, p. 117.

[17] Z. Shi, A. Atrens, *Corros. Sci.* **2011**, *53*, 226.

[18] Z. Shi, J. X. Jia, A. Atrens, *Corros. Sci.* **2011**, *60*, 296.

[19] Z. Qiao, Z. Shi, N. Hort, N. I. Zainal Abidin, A. Atrens, *Corros. Sci.* **2012**, *61*, 185.

[20] Z. Shi, M. Liu, A. Atrens, *Corros. Sci.* **2010**, *52*, 579.

[21] M. C. Zhao, M. Liu, G. Song, A. Atrens, *Corros. Sci.* **2008**, *50*, 1939.

[22] G. Song, A. Atrens, M. Dargusch, *Corros. Sci.* **1999**, *41*, 249.

[23] M. C. Zhao, M. Liu, G. Song, A. Atrens, *Adv. Eng. Mater.* **2008**, *10*, 104.

[24] M. C. Zhao, M. Liu, G. Song, A. Atrens, *Adv. Eng. Mater.* **2008**, *10*, 93.

[25] M. Liu, P. J. Uggowitzer, A. V. Nagasekhar, P. Schmutz, M. Easton, G. Song, A. Atrens, *Corros. Sci.* **2009**, *51*, 602.

[26] M. Liu, P. Schmutz, P. J. Uggowitzer, G. Song, A. Atrens, *Corros. Sci.* **2010**, *52*, 3687.

[27] I. Olefjord, B. O. Elfstrom, *Corrosion* **1982**, *38*, 47.

[28] P. Brüesch, K. Müller, A. Atrens, H. Neff, *Appl. Phys. A* **1985**, *38*, 1.

[29] P. Brüesch, A. Atrens, K. Müller, H. Neff, *Fresenius J. Anal. Chem.* **1984**, *319*, 812.

[30] S. Jin, A. Atrens, *Appl. Phys. A* **1987**, *42*, 149.

[31] R. Kirchheim, B. Heine, H. Fischmeister, S. Hofmann, H. Knote, U. Stolz, *Corros. Sci.* **1989**, *29*, 899.

[32] A. Schneider, D. Kuron, S. Hofmann, R. Kirchheim, *Corros. Sci.* **1990**, *31*, 191.

[33] B. Heine, R. Kirchheim, *Corros. Sci.* **1990**, *31*, 533.

[34] A. S. Lim, A. Atrens, *Appl. Phys. A* **1992**, *54*, 270.

[35] A. S. Lim, A. Atrens, *Appl. Phys. A* **1992**, *54*, 343.

[36] X. Zhang, Z. Zhao, F. Wu, Y. Wang, J. Wu, *J. Mater. Sci.* **2007**, *42*, 8523.

[37] S. Hiromoto, T. Shishido, A. Yamamoto, N. Maruyama, H. Somekawa, T. Mukai, *Corros. Sci.* **2008**, *50*, 2906.

[38] L. Xu, E. Zhang, K. Yang, *J. Mater. Sci.: Mater. Med.* **2009**, *20*, 859.

[39] H. Ardelean, I. Frateur, S. Zanna, A. Atrens, P. Marcus, *Corros. Sci.* **2009**, *51*, 3030.

[40] Z. Shi, G. Song, A. Atrens, *Corros. Sci.* **2005**, *47*, 2760.

[41] Z. Shi, G. L. Song, A. Atrens, *Surf. Coat. Technol.* **2006**, *201*, 492.

[42] Z. Shi, G. L. Song, A. Atrens, *Corros. Sci.* **2006**, *48*, 1939.

[43] Z. Shi, G. Song, A. Atrens, *Corros Sci.* **2006**, *48*, 3531.

[44] P. Liu, X. Pan, W. Yang, K. Cai, Y. Chen, *Mater. Lett.* **2012**, *75*, 118.

[45] Y. Shi, M. Qi, Y. Chen, P. Shi, *Mater. Lett.* **2011**, *65*, 2201.

[46] W. Li, S. Guan, J. Chen, J. Hu, S. Chen, L. Wang, S. Zhu, *Mater. Charact.* **2011**, *62*, 1158.

[47] X. B. Chen, N. Birbilis, T. B. Abbott, *Corros. Sci.* **2011**, *53*, 2263.

[48] P. Salunke, V. Shanov, F. Witte, *Mater. Sci. Eng. B* **2011**, *176*, 1711.

[49] L. Xu, A. Yamamoto, *Colloids Surf. B* **2012**, *93*, 67.

[50] H. Wang, S. Guan, Y. Wang, H. Liu, H. Wang, L. Wang, C. Ren, S. Zhu, K. Chen, *Colloids Surf. B* **2011**, *88*, 254.

[51] G. L. Song, *Prog. Org. Coat.* **2011**, *70*, 252.

[52] X. Yang, G. Wang, G. Dong, F. Gong, M. Zhang, *J. Alloys Compd.* **2009**, *487*, 64.

[53] D. Song, X. Jing, J. Wang, S. Lu, P. Yang, Y. Wang, M. Zhang, *Corros. Sci.* **2011**, *53*, 3651.

[54] Y. Zhang, Y. Shao, T. Zhang, G. Meng, F. Wang, *Corros. Sci.* **2011**, *53*, 3747.

[55] X. Lu, Y. Zuo, X. Zhao, Y. Tang, *Corros. Sci.* **2012**, *60*, 165.

[56] R. G. Hu, S. Zhang, J. F. Bu, C. J. Lin, G. L. Song, *Prog. Org. Coat.* **2012**, *73*, 129.

[57] X. Zhong, Q. Li, J. Hu, X. Yang, F. Luo, Y. Dai, *Prog. Org. Coat.* **2010**, *69*, 52.

[58] N. Scharnagl, C. Blawert, W. Dietzel, *Surf. Coat. Technol.* **2009**, *203*, 1423.

[59] H. Luo, Q. Cai, B. Wei, B. Yu, J. He, D. Li, *J. Alloys Compd.* **2009**, *474*, 551.

[60] S. Hiromoto, M. Tomozawa, *Surf. Coat. Technol.* **2011**, *205*, 4711.

[61] R. Supplit, T. Koch, U. Schubert, *Corros. Sci.* **2007**, *49*, 3015.

[62] J. E. Gray, B. Luan, *J. Alloys Compd.* **2002**, *336*, 88.

[63] A. Mandelli, M. Bestetti, A. Da Forno, N. Lecis, S. P. Trasatti, M. Trueba, *Surf. Coat. Technol.* **2011**, *205*, 4459.

[64] M. R. Barnett, A. Beer, D. Atwell, C. H. J. Davies, T. Abbott, *Magnesium Technology 2010* (Eds: S. A. Agnew, N. R. Neelameggham, E. A. Nyberg, W. H. Sillekens), p. 353.

[65] F. Cao, Z. Shi, J. Hofstetter, P. J. Uggowitzer, G. Song, M. Liu, A. Atrens, *Corros. Sci.* **2013**, *75*, 78.

[66] F. Cao, Z. Shi, G. L. Song, M. Liu, A. Atrens, *Corros. Sci.* **2013**, *76*, 60.

[67] Z. Shi, F. Cao, G. L. Song, M. Liu, A. Atrens, *Corros. Sci.* **2013**, *76*, 98.

[68] L. Müller, F. A. Müller, *Acta Biomater.* **2006**, *2*, 181.

[69] S. Verdier, M. Boinet, S. Maximovitch, F. Dalard, *Corros. Sci.* **2005**, *47*, 1429.